Degradation of chlorinated and hydroxylated intermediates in UVA/ClO$_2$ systems: A chlorine-based advanced oxidation process investigation

Daniele Scheres Firak, Luca Farkas, Máté Náfrádi, Tünde Alapi [*]

University of Szeged, Department of Inorganic and Analytical Chemistry, Dóm tér 7, Szeged H-6720, Hungary

ARTICLE INFO

ABSTRACT

The chlorination used in water treatment plants can promote the formation of toxic compounds, which can be minimized by substituting free available chlorine (FAC) with chlorine dioxide (ClO$_2$). Besides disinfection, combining ClO$_2$ with UV radiation leads to the efficient elimination of organic substances. This work employed a lab-made reactor equipped with LEDs emitting at 367 nm with adjustable photon flux to investigate the efficiency of the UVA/ClO$_2$ process and the formation of hydroxylated and chlorinated products during the degradation of phenol and coumarin. The degradation of coumarin was investigated in a central composite design and depended on the ClO$_2$ concentration and pH. Increasing the ClO$_2$ concentration was necessary to promote the degradation. In higher ClO$_2$/phenol ratios, 80% of the total phenolic compounds were removed at pH 3, 5.5, and 8. The mineralization efficiency increased with the pH, along with the concentration of chlorinated compounds, indicating these products are more persistent than the hydroxylated ones. The UVA/ClO$_2$ process was advantageous in removing and mineralizing phenol and coumarin if compared to direct oxidation, but the process needs to be improved to minimize the formation of chlorinated organic products, and elimination of ClO$_2^-$ and ClO$_3^-$ requires post-treatment method.

1. Introduction

Chlorination is widely used in water treatment plants in different treatment stages, controlling algae blooms, assisting in coagulation, and promoting or ensuring disinfection [1]. One of the significant drawbacks of this practice is the formation of toxic chlorinated organic compounds formed in the presence of natural organic matter and labile organic matter. For instance, the chlorination of phenols leads to the formation of chloroform and other chlorinated compounds, which increase the toxicity of the treated water [2,3]. For reducing the formation of chlorination of organic compounds, free available chlorine (FAC) species were replaced with other chlorine sources, such as chlorine dioxide (ClO$_2$) [1,4].

The biggest drawback of ClO$_2$ is the need for on-site generation since it is an unstable species, easily decomposed into chlorine and oxygen in the presence of radiation or a heat source. Furthermore, ClO$_2$ cannot be compressed or commercially stored because it is explosive at concentrations higher than 10% in the air [5]. There are, however, several reactions that lead to the formation of small concentrations of dissolved ClO$_2$ that can be safely and efficiently prepared both in a laboratory and

in large scales, including the reaction between sodium chlorite and sulfuric acid [6], sodium chlorite and persulfate [7], chlorite ion and hypochlorous acid, sodium chlorite and chlorine gas [1], among many others. As long as the ClO$_2$ is formed in situ and in conditions that avoid its volatilization, it can be safely dosed and mixed with water. These requirements are easily met at environmental conditions since ClO$_2$ is highly water-soluble (at 25 °C its solubility is about 70 g/L) [1]. The most important aspect for this application is the method used to introduce ClO$_2$ in the reactor, which cannot be performed upstream, in open pipes, or with rapid mixing to avoid ClO$_2$ escaping to the atmosphere [1].

ClO$_2$ is a selective oxidant that has been investigated in the direct oxidation of micropollutants [11] and natural organic matter [10], and it was found to be more reactive towards electron-rich groups, such as phenols and anilines, and less reactive towards primary and secondary amines [11]. In general, the direct oxidation of organic compounds occurs through electron transfer reactions, and ClO$_2$ can be reduced to Cl$^-$ in the presence of reductive substances [12]. Although ClO$_2$ has been used as a disinfectant in water treatment plants since the 70's [1], applications are limited to the direct oxidation. However, the reactivity of

ClO_2 can be modified with exposure to UV radiation, in the processes known as UV/ClO_2. The mechanisms for the formation of reactive species in UV/ClO_2 processes have been investigated mainly in the gas phase due to its importance for the ozone layer depletion [13], while investigations using pump-probe Raman and resonance Raman spectroscopy in the aqueous phase have been used to study the photodissociation of ClO_2 [14,15]. It is accepted that the ClO_2 molecule undergoes photodissociation processes that lead to the formation of the primary radicals oxygen ($O^\bullet$), chlorine ($Cl^\bullet$), and chlorine oxide ($ClO^\bullet$) according to reactions (1) and (2) [14–17]. Recently, the photolysis of ClO_2 under 365 nm LED irradiation was investigated in studies using femtosecond transient absorption spectroscopy [18], and reactions (1) and (2) were found to form different products. The main products of the chain initiated by reaction (1) were ClO_3^- and Cl^-, while reaction (2) resulted in ClO_3^-, Cl^- and also FAC. The photolysis of ClO_2 is strongly affected by the vibrational-relaxation dynamics of the molecule, and the radical species are modified with changes in the applied wavelength and solvent properties [14,15]. The radical oxygen can lead to hydroxyl radical ($HO^\bullet$) formation in aqueous media, and the UV/ClO_2 process can, therefore, be used to degrade organic compounds using both reactive oxygen species (ROS) and reactive chlorine species (RCS) [16, 18].

$$ClO_2 \xrightarrow{h\nu} ClO^\bullet + O^\bullet \quad \Phi = 0.05 \ (365 \ nm) \tag{1}$$

$$ClO_2 \xrightarrow{h\nu} Cl^\bullet + O_2 \quad \Phi = 0.17 (390 \ nm) \tag{2}$$

$$ClO^\bullet \xrightarrow{h\nu} Cl^\bullet + O^\bullet \tag{3}$$

$$O^\bullet + H_2O \ \rightarrow \ 2 \ HO^\bullet \quad k = 1.8 \times 10^{10} \ M^{-1} \ s^{-1} \tag{4}$$
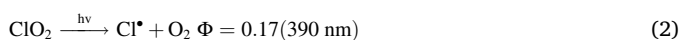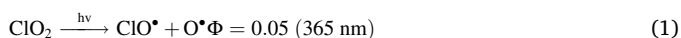
The reaction mechanism above shows that the UV/ClO_2 process forms $Cl\bullet$ ($E^0 = 1.90$ V vs. NHE [19]), $ClO\bullet$ ($E^0 = 1.41$–1.8 V vs. NHE [19]) and $O\bullet$ ($E^0 = 2.42$ V vs. NHE [19]) as primary radicals and $HO\bullet$ ($E^0 = 2.73$ V vs. NHE [19]) as secondary radicals. The RCS are selective reaction partners; their reactivity depends on pH [20]. While $HO\bullet$ are nonselective species. $Cl\bullet$ reacts mainly with substituted aromatics, such as phenolic compounds, and $ClO\bullet$ reacts primarily with phenolates and methoxybenzenes [20,21]. In a recent study, $ClO\bullet$ was shown to be the main reactive species participating in the degradation of polychloro–1, 3–butadienes in UV/Chlorine processes [22]. The contribution of $HO\bullet$ and $Cl\bullet$ to the degradation of micropollutants in UV/Chlorine systems decreases at increasing pH values due to scavenging effects of ClO^-, which is not observed for $ClO\bullet$ [20]. The scavenging effect of ClO^- can also be relevant in UV/ClO_2 systems since the formation of FAC is usually reported in the presence of ClO_2 [12,23]. However, the presence of FAC can also assist in the degradation of certain organic compounds, as recently described in a study investigating the degradation of ciprofloxacin in UV/ClO_2 [24]. Besides RCS and $HO\bullet$, singlet oxygen ($^1O_2$) was also reported to participate in the degradation of organic compounds [25]. All these different reactive species can be important to promote the degradation of pollutants at different reaction conditions.

Also essential to ensure the applicability of UV/ClO_2 processes is the source of radiation. With the growing availability of LED lamps in the market, the interest in applying these light sources in photocatalytic processes has increased, and different applications for water treatment have been reported, including the use of LED in heterogeneous photocatalysis with TiO_2 [26], water disinfection systems [27,28], and chlorine-based AOPs [29,30]. LED lamps in photocatalytic rectors present several advantages over the traditional mercury vapor lamp systems. The main advantages include the longer lifetime of the LEDs (which can be 5 times longer than the Hg vapor lamps), the higher energy efficiency, the possibility of selecting different wavelengths, the absence of a warm-up time (as typically seen in Hg vapor lamps), and finally, the possibility of adapting the LED lamps to different reactor shapes and settings [26,31]. In the case of UV/ClO_2 processes, the use of LED lights permits the selection of wavelengths that are much closer to the absorption maximum of ClO_2 ($\varepsilon^{359 \ nm} = 1230$ M^{-1} cm^{-1}) [11] than 254 nm monochromatic UV light emitted by low-pressure mercury vapor lamp.

Recent studies have demonstrated that chlorine-based AOPs present similar or superior performances in comparative water treatment studies using UV/Chlorine, UV/H_2O_2, and $UV/S_2O_8^{2-}$ [19,32]. The costs associated with electric energy and chemicals are usually lower in UV/Chlorine processes than UV/H_2O_2, and change with the pH and the chemical structure of the target compounds [19]. The most significant drawback of the chlorine-based AOPs compared to the processes based exclusively on $HO\bullet$ or $SO_4^{\bullet-}$ is the formation of chlorinated organic products, chlorite (ClO_2^-), and chlorate (ClO_3^-) ions. ClO_2^- and ClO_3^- present toxicity and should be limited to 0.7 mg L^{-1} in drinking water according to World Health Organization guidelines [33]. Their amount depends on the degradation mechanisms of the organic compounds, their reactivity towards RCS, and the pH of the treated solution [19,32].

The primary purpose of this work is to apply the already broadly used ClO_2 in UVA/ClO_2 processes for the degradation of coumarin and phenol and investigate the formation and degradation of chlorinated products in a lab-scale reactor equipped with LED emitting at 367 nm. Coumarin (COU) is frequently used as a fragrance in personal care products [34] and investigated as a probe for $HO^\bullet$ in AOPs. Its hydroxylated product, 7-hydroxycoumarin (7OH-COU), is highly fluorescent (emission at 450 nm), and can be determined by fluorescence spectroscopy with a low limit of detection [35]. Phenol is a good candidate for target compound since humic materials present in water are mainly formed by monohydroxy-benzenes that can react with chlorine and form trihalomethanes (THM) [2]. Furthermore, it can easily undergo chlorination, and its degradation products have already been identified both in the presence of FAC and ClO_2 [2,36,37]. Therefore, the phenol degradation and the monitoring of chlorinated by-products, ClO_2^- and ClO_3^- can be used to attest to the viability of chlorine-based AOPs.

2. Material and methods

2.1. Reactor and reactions conditions

Reactions were conducted in a lab-made LED reactor with 12 LEDs emitting at 367 nm, fixed in 6 adjustable cooling plates. The LED reactor was built using surface-mounted diodes (SMD) emitting at 367 nm (Vishay; VLMU3510–365–130; 4.0 V opening voltage, 690 mW radiant power at 500 mA). 12 SMD were soldered on metal core printed circuit boards (MCPCB, supplied by Meodex) and fixed on aluminum heat sinks (Fischer Elektronik; 0.70 K W^{-1}). A power supply (Axiomet; AX-3005DBL-3; maximum output 5.0 A / 30.0 V) was used to provide and control the electrical power needed to operate the light sources. The aluminum heat sinks can be moved to provide different reactor configurations. The configuration used was the opposite heat sinks at 9 cm from each other (LED reactor diameter), with a 100 mL glass vessel closed with a PTFE cap placed at the center of the reactor. The glass vessel cap was adapted with a PTFE hose for sampling. A picture of the reactor and a schematic representation is shown in Fig S1. Different LED powers were used during the experiments, adjusted with different electrical currents. The photon fluxes in each current were determined using ferrioxalate actinometry, described in the Supplementary Information.

The reaction pH was controlled with phosphate buffer 20 mM (K_2HPO_4 99% from Acros Organics and KH_2PO_4 HPLC grade from VWR). Free radicals and oxidants were quenched with sodium thiosulfate ($S_2O_3^{2-}$) after sampling, added to the samples in a concentration 5 times higher than the initial ClO_2 concentration. Samples were bubbled with nitrogen after the addition of thiosulfate to remove residual ClO_2 and possible oxidants formed as dissolved gases.

Chlorine dioxide was prepared in water with a commercial additive (TwinOxide®). TwinOxide® reagents, $NaClO_2$ and $NaHSO_4$, were mixed

in an amber flask and kept in the dark for 3 days before use. Because ClO_2 is more stable in aqueous media at acidic pH [7,8], this reaction (5 (5)) results in ClO_2 solutions that can be stored for an extended period [9,10].

$$5NaClO_2 + 5NaHSO_4 \rightarrow 4ClO_2 + HCl + 5Na_2SO_4 + 2H_2O \qquad (5)$$
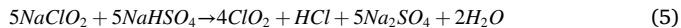
The final ClO_2 concentration was monitored daily using the DPD-glycine ClO_2 method from Hach®. The ClO_2 solutions were refrigerated, shielded from light, and stable for about a month, following the manufacturer's recommendations [38]. The DPD test was also used to determine FAC (VWR, sodium hypochlorite, 14% Cl_2).

2.2. Central composite design experiments

A central composite design (CCD) was used as a screening tool to investigate the degradation of COU (Sigma, $\geq$ 99%, HPLC) and the formation of the hydroxylated product 7OH-COU in the LED reactor. The following table shows the settings selected for the factors pH, the concentration of ClO_2, and LED power (converted to photon flux with the ferrioxalate actinometry, Fig S2, and Table S1). The initial temperature of the reactions was set to 20 $\pm$ 1 ºC, and the final temperature was monitored to assess changes in the temperature of the reaction vessel related to the electronic components of the LED reactor.

2.3. Analytical methods

The formation of 7OH-COU was monitored with a Hitachi F-4500 fluorescence spectrometer, with excitation wavelength set at 345 nm and emission at 455 nm. Excitation and emission slits were 5 nm, and the scan was 600 nm s^{-1}. The conversion rate of COU was determined from the change of absorbance at 277 nm, the characteristic wavelength of the absorption spectrum of COU. Spectra were measured with UV–vis spectrometer (Agilent 8453). Degradation products were identified in an Agilent 6890 N gas chromatographer with a 5973 N single quadrupole mass spectrometer (mass spectral library NIST02). A HB-5 MS capillary column (30 m × 320 mm × 0.5 mm film thickness) was used in the chromatographic method. The column oven was programmed from 60 ºC (1 min) to 275 ºC at a rate of 20 ºC min^{-1}. Electron impact (EI) mode was set at 70 eV, and the scan range from 10 to 350 *m/z*. Sample preparation was done in Strata™-X 33 μm polymeric sorbent (60 mg) SPE columns, with preconcentration factors of 100. After the SPE elution, 25 μM of 4–4′-biphenol (BIP, 97%, Aldrich) were added to the samples as internal standard.

The degradation of phenol (VWR, AnalaR NORMAPUR®, 99–100.5%) and formation of hydroxylated phenols were monitored in a UV–visible spectrophotometer (Agilent 8453) using the Folin-Ciocalteu method (FC, Folin-Ciocalteu's reagent VWR for analysis of total phenolic compounds, TPC) [39]. In this colorimetric method, 0.5 mL of a sample is diluted to 2 mL, and later 0.5 mL of a carbonate-tartrate buffer (100 g L^{-1} Na_2CO_3 and 6 g L^{-1} $Na_2C_4H_4O_6$) is added to the sample, followed by 50 μL of the FC reagent. The sample is vigorously shaken and later allowed to stand for 30 min in the dark, forming a blue-colored complex with maximum absorbance at 760 nm. The wavelength of the maximum absorbance can vary with the concentration of phenolic compounds. The calibration curve for total phenols was done with gallic acid and read at 730 and 760 nm, presenting a linear range from 0.5 to 50 mg L^{-1}. Identification of chlorinated phenols and hydroxylated species resulting from the degradation of phenol in UV/ClO_2 processes was conducted in the same GC-MS system mentioned in the previous section. The column oven was programmed from 40 ºC (1 min) to 275 ºC at a rate of 20 ºC min^{-1}. Total Organic Carbon (TOC) was monitored using a TOC analyzer (Analitik Jena, Multi N/C). Adsorbable organic halogens (AOX) were quantified in an AOX analyzer (Analytik Jena, Multi X 2500) using the column method with adsorption in quartz containers filled with activated carbon. Samples were prepared in a sample preparation module (Analytik Jena, APU 2).

The formation of inorganic anions (Cl^-, ClO_2^-, ClO_3^-) was measured using ion chromatography (Shimadzu Prominence LC—20 CE, Shodex NI—424 5 U column). The eluent was 2.3×10^{-3} M aminomethane with a flow rate of 1.0 cm^3 min^{-1}.

Ecotoxicity tests (LCK480, Hach-Lange) were based on the bioluminescence inhibition of the marine bacteria *Vibrio fischeri*. The bioluminescence of the test organism was measured using a Lumistox 300 (Hach Lange) luminometer after 15 and 30 min incubation time.

3. Results and discussion

3.1. Central composite design

The degradation of COU and the formation and consumption of 7OH-COU were used to optimize the reaction parameters. A central composite design (CCD) was built to screen the variables ClO_2 concentration, pH, and photon flux. The three independent variables were investigated in the levels described in Table 1.

Using the degradation percentage of COU as the answer for the CCD, it was possible to generate a model in which only the linear main effects of pH and ClO_2 concentration were significant (p-values 0.014 and 0.0026, respectively). The ANOVA table (Table S4), Pareto chart of effects, and the plot of observed versus predicted values can be seen in the Supplementary Information (Fig S3a and S3b). The main results of the CCD are illustrated by the following fitted surface (Fig. 1b). Modifying the photon flux did not significantly affect the answer, and similar fitted surfaces are generated at different levels for this variable (Fig S3c).

According to the CCD responses, an optimal operational condition is found at the standard values for pH and LED (pH = 5.5 and photon flux of 1.26×10^{-5} mol$_{photon}$ L^{-1} s^{-1}), but more ClO_2 needs to be added to the reactions to promote the degradation. The maximum degradation percentages after one hour were achieved in runs 6 (25.88 $\pm$ 2.35%; ClO_2/pH/LED = +1/−1/+1, ClO_2 = 20 mg L^{-1}, pH = 3, φ = 1.85×10^{-5} mol$_{photon}$ L^{-1} s^{-1}) and 10 (25.81 $\pm$ 2.35%; ClO_2/pH/LED = +1/0/0, ClO_2 = 20 mg L^{-1}, pH = 5.5, φ = 1.26×10^{-5} mol$_{photon}$ L^{-1} s^{-1}) (Table S2). It is worth noting that, to achieve similar efficiencies, the electrical power requirements of run 6 are more than twice that of run 10.

The concentration 7OH-COU, a hydroxylated product of COU, was monitored to obtain information about the effect of the variables on the HO• formation. Still using the variable levels shown in Table 1, another CCD model was built using the maximum concentration of 7OH-COU as the dependent variable. The pH was the major significant variable in the model (p < 0.01), and the higher 7OH-COU concentrations were determined at pH 3 (Fig. 1c). The photon flux (p = 0.055) also affected the answers (Tables S3 and S5). The higher concentration of 7OH-COU was 1.19($\pm$ 0.08) $\times 10^{-6}$ mol L^{-1} achieved in run 11 (ClO_2/pH/LED = +1/−1/0, Table S3), at the higher level for the variable concentration of ClO_2 (20 mg L^{-1}), lower level for pH (pH = 3), and standard level for the photon flux (1.26×10^{-5} mol$_{photon}$ L^{-1} s^{-1}). Similar answers were achieved for runs 1, 2, and 6; all performed at pH 3. The response surface of this new CCD model shows that the concentration of ClO_2 did not significantly affect the answer, and, therefore, only the fitted surface for the standard value for this variable is presented in Fig. 1d (the fitted surfaces for the other levels are shown in Fig S4c).

The fact that the maximum responses for the two investigated dependent variables are achieved at different conditions – we have a

Table 1
Factor level settings for the degradation of coumarin.

	Low (−1)	Standard (0)	High (+1)
[ClO_2] (mg L^{-1})	8	14	20
pH	3	5.5	8
LED power (W)	1.4	3.7	6.4
(photon flux (mol$_{photon}$ L^{-1} s^{-1}))	9.12×10^{-6}	1.26×10^{-5}	1.85×10^{-5}
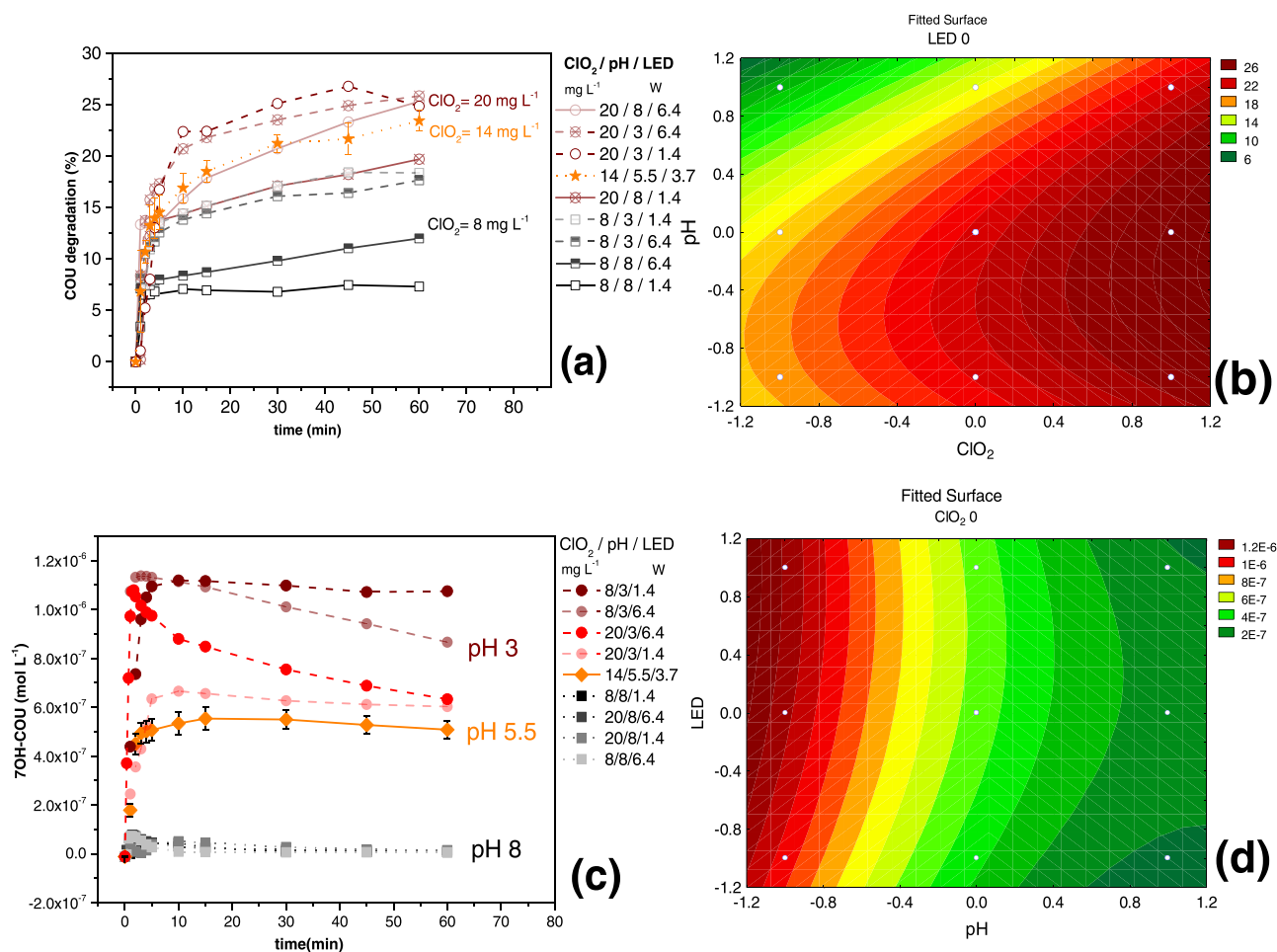
Fig. 1. Kinetic profile of the COU degradation (a) and 7-OH-COU formation (c) in the conditions specified in the CCD and response surfaces (b: COU degradation affected by the factors pH and ClO_2 concentration (photon flux: 1.26×10^{-5} mol_{photon} L^{-1} s^{-1}); d: 7-OH-COU formation affected by the factors LED photon flux and pH (ClO_2: 2.08×10^{-4} M (14 mg L^{-1})).

maximum degradation of COU at higher concentrations of ClO_2 and higher pH values but a maximum formation 7OH-COU at lower pH values – indicates the HO• addition is probably not the primary mechanism for the degradation of COU. 7OH-COU formation is often used as an indicator for the HO• formation in AOPs [40–45]. However, in addition to 7OH-COU, other hydroxylated products are also formed. [46,47] The mechanisms that lead to the formation of the hydroxylated products depend on reaction conditions [47].

The products of the COU degradation were monitored in a GC-MS. After five additions of 2.08×10^{-4} M (14 mg L^{-1}) of ClO_2 and irradiation at 3.7 W, similar products were observed at pH 3 and 5. Three main degradation pathways (illustrated in Fig. 2) consist of a nucleophilic attack on the carbonyl group of the lactone ring, which causes the opening of this structure or the addition of HO• and Cl• to the benzene ring. According to Louit et al., positions 3–8 of the COU structure (indicated in Fig. 2) are subjected to hydroxylation [46]. The UVA/ClO_2 process appears to generate equal amounts of hydroxylated products in positions 7 and 8, and smaller amounts of coumarins hydroxylated in position 6. Huang et al. investigated the chlorination of COU in UV/peroxymonusulfate (UV/PMS) reactions in the presence of chloride ions [48] and proposed the 3-chloroisocoumarin as the dominant chlorinated product. In the UVA/ClO_2 process, however, different radical species, particularly the Cl• and ClO• can affect the formation of chlorinated products. Furthermore, the products derived from the ring-opening are predominant in the reactions (Fig. 2), affecting the formation of both the hydroxylated and the chlorinated products.

3.2. Effect of successive additions of ClO_2 on COU conversion

Considering the responses of the CCD for the experiments of COU degradation, it was evident that further addition of ClO_2 would be required to complete the degradation. The ClO_2 photodissociation was investigated under the same conditions parallel to the CCD experiments. A fast consumption of 14 mg L^{-1} ClO_2 was observed within less than 5 min. Comparing the results obtained for the degradation of COU (Fig. 1a) with the photodissociation of ClO_2, it can be noticed that the time required for the ClO_2 photodissociation corresponds to the fast degradation of COU in all conditions. Therefore, we opted to increase the concentration of ClO_2 in successive additions. The time required for ClO_2 degradation did not change with successive doses (Fig. 3). Therefore, the intermediate level for the variable photon flux and five consecutive additions of ClO_2 were considered in subsequent experiments targeting the degradation of organic compounds.

At the three investigated pH, with 5 successive additions of ClO_2, over 50% (pH 3 = 51%, pH 5 = 57%, and pH 8 = 62%) of the COU ($[COU]_0 = 1.0 \times 10^{-4}$ M) was converted to by-products after 60 min in the presence of radiation, while the degradation by ClO_2 without radiation was around 10% (pH 3 = 7%, pH 5 = 10%, and pH 8 = 12%). The organic carbon removal and the AOX formation given as percentage of chlorinated carbon structures (Cl-C) are shown in Fig. 4. (The values used for calculation are shown in Table S6).

A few chlorinated products, deriving from Cl• addition formed after the lactone ring-opening, were detected at pH 3 and 5.5 (Fig S5). The resulting chlorinated products are recalcitrant to further oxidation,
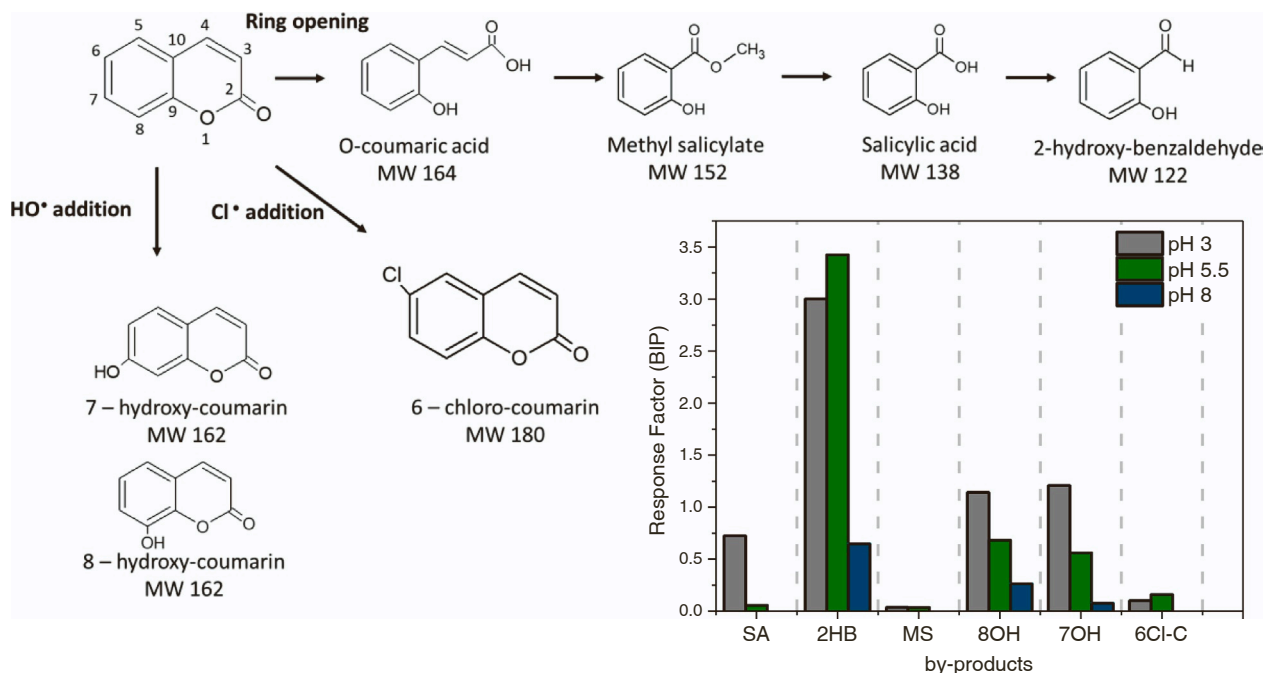
Fig. 2. Degradation mechanism of COU showing the ring-opening and the addition of •Cl and •OH radicals and response factor for the main by-products (inserted Figure) observed during the degradation of COU in UVA/ClO$_2$ processes. SA: salicylic acid; 2HB: 2-hydroxybenzaldehyde; MS: methyl salicylate; 8OH: 8-hydroxy coumarin; 7OH: 7-hydroxy coumarin; 6Cl-C: 6-chloro coumarin. Conditions: [COU]$_0$ = 1.0 × 10^{-4} M, 5 × [ClO$_2$]$_0$ = 2.08 × 10^{-4} M (14 mg L^{-1}), photon flux = 1.26 × 10^{-5} mol$_{photon}$ L^{-1} s^{-1}.
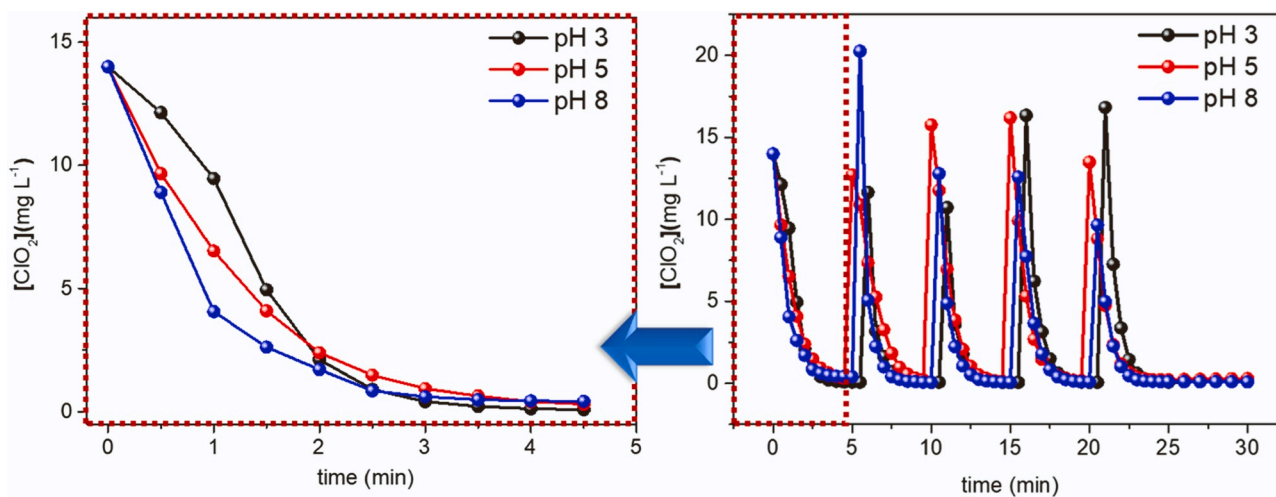
Fig. 3. Photolysis of ClO$_2$ under 367 nm at different pH. Concentrations were obtained using the absorbance monitored at 359 nm. Conditions: 5 × [ClO$_2$]$_0$ = 2.08 × 10^{-4} M (14 mg L^{-1}).

causing the rise in Cl-C percentage (Fig. 4). At pH 8, however, 2-hydroxy-benzaldehyde was the major product, both in the presence and absence of UV radiation. This indicates that the attack to the carbonyl group is preferred at pH 8, which also explains the higher carbon removal observed at this pH.

The experiments were repeated in the presence of tert-butyl alcohol (TBA) (Fig. 5). Although TBA is usually used as a HO• scavenger, it can also react with RCS ($k_{TBA-HO•}$ = 6.0 × 10^8 M^{-1} s^{-1}, $k_{TBA-Cl•}$ = 3.0 × 10^8 M^{-1} s^{-1}, $k_{TBA-ClO•}$ = 1.3 × 10^7 M^{-1} s^{-1}) [20]. The initial TBA concentration used in this study was 100 times higher than the COU concentration to assure that a significant fraction of HO• (0.96; Supplementary Information, ES2) reacts with TBA instead of COU ($k_{COU-HO•}$ = 2 × 10^9 M^{-1} s^{-1} [45]). The degradation rate of COU decreased in the UVA/ClO$_2$ system (Figs. 5 and S6a) at all investigated pH. The simultaneous

reduction in the concentrations of 7OH-COU at pH 3 and 5.5 (Fig S6b) was also observed. The highest COU conversion rate was measured at pH 8, but with negligible 7OH-COU formation. However, the addition of TBA reduced the COU degradation at pH 8 to a similar value as at pH 3 and pH 5.5.

Similar studies were conducted by Tian et al., who investigated the degradation of iopamidol by different UV-induced processes, including UVC/ClO$_2$ with low-pressure mercury vapor lamps (emission at 254 nm) [16]. The authors observed an increase in the rate constant for the degradation of iopamidol at higher pH values (from pH 5–9) and proposed O• to be the dominant species in the process since the addition of TBA did not significantly modify the degradation rate [16]. The reactions with ClO• and O• can also play an essential role in degrading organic compounds in the UVA/ClO$_2$ system. Considering these
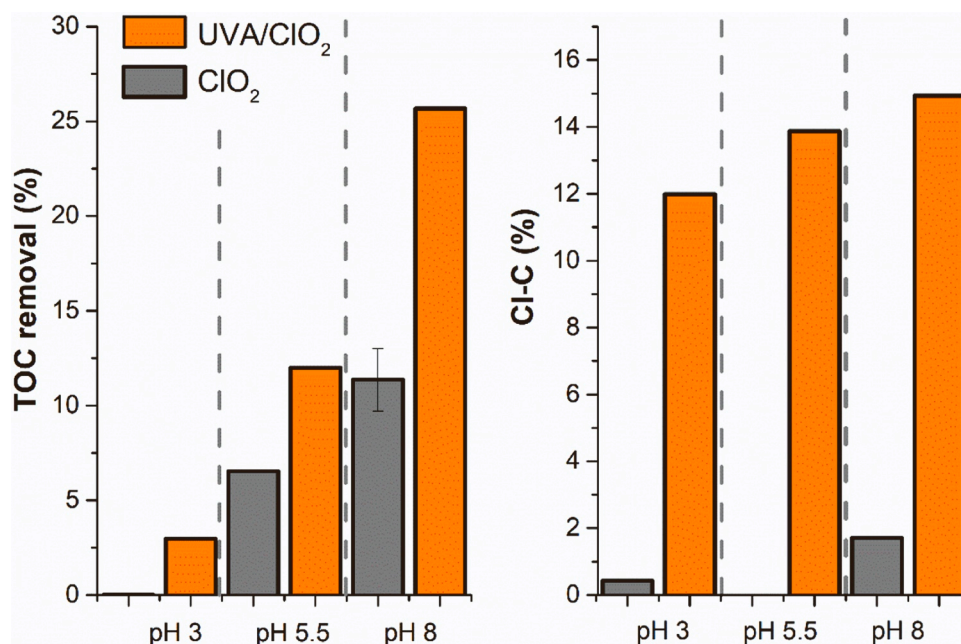
Fig. 4. TOC removal and AOX formation in COU degradation. Conditions: $[COU]_0 = 1.0 \times 10^{-4}$ M, $5 \times [ClO_2]_0 = 2.08 \times 10^{-4}$ M, photon flux $= 1.26 \times 10^{-5}$ mol_{photon} L^{-1} s^{-1}. (Cl-C: chlorinated carbon structures; AOX value divided by the TOC value).
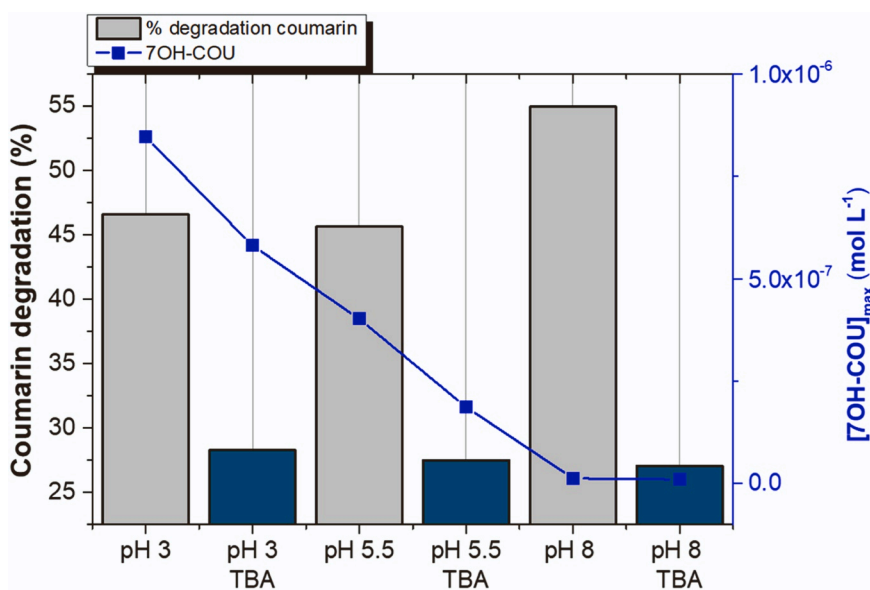
Fig. 5. Degradation of COU and formation of 7OH-COU in experiments conducted in the presence of TBA after 30 min. ($[COU]_0 = 1.0 \times 10^{-4}$ M, $[TBA]_0 = 1.0 \times 10^{-2}$ M, $5 \times [ClO_2]_0 = 2.08 \times 10^{-4}$ M, photon flux $= 1.26 \times 10^{-5}$ mol_{photon} L^{-1} s^{-1}).

degradation patterns, the CCD results, and TBA effect, we can infer that the formation and contribution of ROS and RCS in UVA/ClO$_2$ systems is strongly affected by the pH, and HO• are more likely to take part in hydroxylation reactions conducted at lower pH values. Therefore, further investigations are necessary to estimate the contribution of each radical species to the formation of hydroxylated and chlorinated products at different pH values.

3.3. Degradation of phenol

In contrast to COU, phenol can easily be directly oxidized by ClO$_2$. The mechanism of phenol degradation by ClO$_2$ depends on the phenol: ClO$_2$ ratio. Wajon et al. observed that ClO$_2$ must be applied in excess to avoid the formation of chlorinated phenols [36]. According to these authors, the rate-limiting step in the direct oxidation would be the formation of phenolate after hydrogen abstraction by ClO$_2$, which forms p-benzoquinone and HOCl. The HOCl further reacts with phenol and benzoquinone to form chlorinated species. In the present work, preliminary experiments were conducted with a 1:1 ClO$_2$:phenol ratio, with 0.5 mM of phenol and 5 successive additions of 0.1 mM (8 mg L^{-1}) ClO$_2$. Experiments were conducted in 120 min, both in the absence (in the dark) and the presence of UVA. In the absence of radiation, the direct oxidation by ClO$_2$ resulted in 27% degradation at pH 3, but no significant degradation was observed at pH 5.5 and 8. The main products were p-benzoquinone and chlorinated phenols. The UVA irradiation enhanced the phenol degradation, and improved efficiency with

increasing pH was observed (50%, 70%, and 63% removal after 120 min for pH 3, 5.5, and 8, respectively). Moreover, the product distribution also changed (Fig S7) compared to the direct oxidation by ClO_2. The number of detected halogenated products increased significantly, clearly due to RCS-initiated reactions formed via UVA photolysis of ClO_2.

3.4. Effect of successive additions of ClO_2 on phenol conversion

The increase in the oxidant concentration would increase the degradation of organic compounds. Thus, the ClO_2:phenol ratio was increased to 20 with successive additions of 14 mg L^{-1} ClO_2 to 50 μM of phenol. In this way, the phenol was removed completely, and the TPC showed an 80% removal for all tested pH in the presence of radiation (Fig. 6a). In contrast, in the absence of radiation, an increase in the TPC

was observed due to the formation of polyhydroxylated and chlorinated phenols. Since the FC reagent reacts with phenols, phenolic compounds with more than one hydroxyl group have a higher response in this test. Fig. 6a indicates that direct oxidation reactions are less efficient than the UVA/ClO_2 process since the hydroxylation of phenol is not followed by the cleavage of the aromatic ring.

The TPC monitoring agreed with the TOC results (Fig. 6b): the carbon removal is more efficient in the presence of radiation. The TOC removal after one hour is similar (less than 15%) at each pH in the absence of radiation but increases with the increase of pH in the case of UVA/ClO_2 process (Fig. 6b), similarly to that observed in the case of COU (Fig. 4). Because the UVA/ClO_2 reaction takes place immediately after the addition of ClO_2 (added ClO_2 decomposes within 5 min (Fig. 3)), no more than 10% further TOC decrease was achieved from 30 min (time necessary to reduce TPC as seen in Fig. 6a) to 60 min,
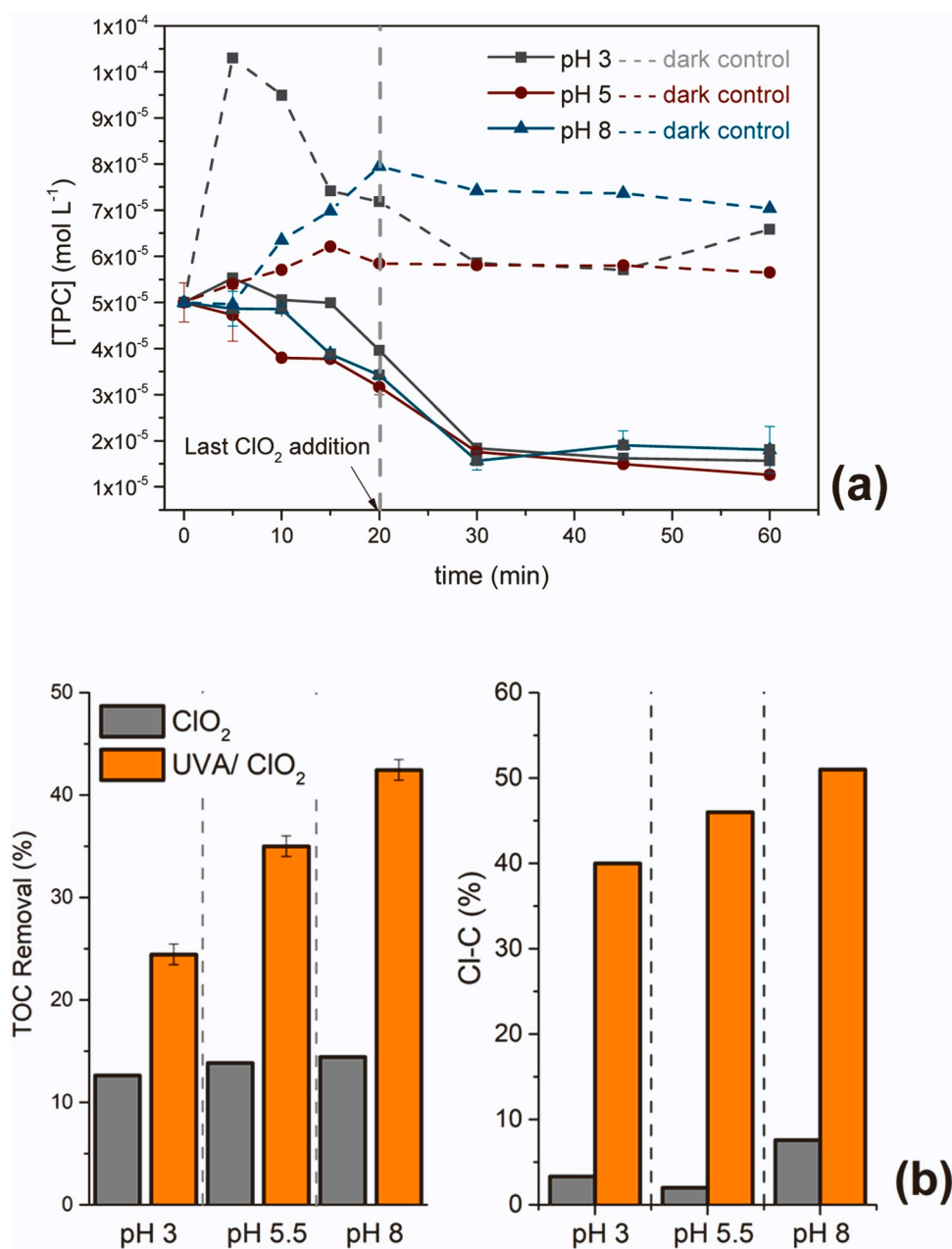
Fig. 6. TPC removal (a), TOC removal (b) and percentage of chlorinated carbon structures (concentration of AOX (mg^{Cl} L^{-1} divided by the concentration of TOC (mg^C L^{-1} determined after 60 min) (c) in the degradation of phenol (ClO_2/phenol = 20; 5 ×$[ClO_2]_0$ = 2.08 × 10^{-4} M (14 mg L^{-1}), $[phenol]_0$ = 5 × 10^{-5} M, photon flux = 1.26 × 10^{-5} mol$_{photon}$ L^{-1} s^{-1}).

which can be attributed to reactions with the by-products.

The speciation of phenol can play an important role in direct oxidation reactions. According to Lee and von Gunten (2010), the direct oxidation of phenol is faster at higher pH values because phenolate has a significantly higher reaction rate constant with ClO_2 ($k_{phenol-ClO2}$ = 0.24 M^{-1} s^{-1}, $k_{phenolate-ClO2}$ = 2.7 × 10^7 M^{-1} s^{-1}) [11]. The transformation rate increases with the phenolate fraction, as shown in Table S7 and Fig S8. At pH 8, the calculated rate constant is 10^6 times higher (k_{pH8} = 4.27 × 10^4 M^{-1} s^{-1}) than the constant related to the reaction of phenol with ClO_2 (k_{phenol} = 0.24 M^{-1} s^{-1}). Besides the phenol speciation, the formation of active radicals during the ClO_2 dissociation is also crucial for direct oxidation. Marcon et al. investigated the decomposition of ClO_2 using electron paramagnetic resonance spectroscopy and observed that the decomposition of ClO_2 produces HO• [6].

Fig. 6b also shows the percentage of halogenated carbon structures calculated using the TOC and AOX values determined after 1 h of treatment (Table S8). In the UVA/ClO_2 process, the TPC removal is similar at each investigated pH, while the carbon removal efficiency and the percentage of the chlorinated products increase with the pH (Fig. 6b). These are consistent with the observation made in the case of the COU transformation, which indicates the UVA/ClO_2 process generated radicals that are not selective to the investigated degradation substrates. Since HO• reacts at diffusion-controlled rates with phenol ($k_{OH-phenol}$ = 1.0 × 10^{10} M^{-1} s^{-1}[11]), Cl• is selective to substituted aromatics, and ClO• to phenolates [20], the degradation of phenol should occur at all investigated pH. However, as shown in Fig. 6b, the direct oxidation by ClO_2 is not efficient in reducing the TOC content. The

increase of TPC and the low AOX values indicate that the hydroxylation of phenol is more favoured without irradiation. The products confirmed all these findings: phenol was converted into hydroquinone, p-benzoquinone, hydroxylated products, and salicylic acid, which agrees with previously reported mechanisms for the direct oxidation of phenol by ClO_2 [36]. At pH 3, however, chlorinated structures such as 2-chloro-1,4-benzenediol were also observed. A summary of the main structures detected at different pH during the degradation of phenol via direct chlorination and in the UVA/ClO_2 system is shown in the Supplementary Information (Table S9).

Phenol degradation experiments were repeated in the presence of TBA to investigate the contribution of active radicals in the removal of TPC (Fig. 7). The TBA appears to have more interference in the direct oxidation of phenol conducted at pH 3 and 5.5, which could indicate hydroxylation occurs through the addition of HO• radicals, as described in the work of Marcon et al. [6] that proposed the formation of HO• in the presence of ClO_2. The presence of TBA caused a slight decrease in the rate of TPC removal during the UVA/ClO_2 at pH 8. However, the TPC profile was not significantly affected by TBA at pH 3 and 5.5. The TPC increase at pH 8 was not affected by the presence of a radical scavenger, which confirms that the hydroxylation mechanisms at alkaline pH can be caused by direct oxidation and not a radical-based mechanism.

3.5. The role of FAC on phenol conversion

Since ClO_2 is completely removed within 5 min (Fig. 3), further degradation can occur via the formation of FAC species. Rouge et al. (2018) demonstrated that FAC could be generated in situ during
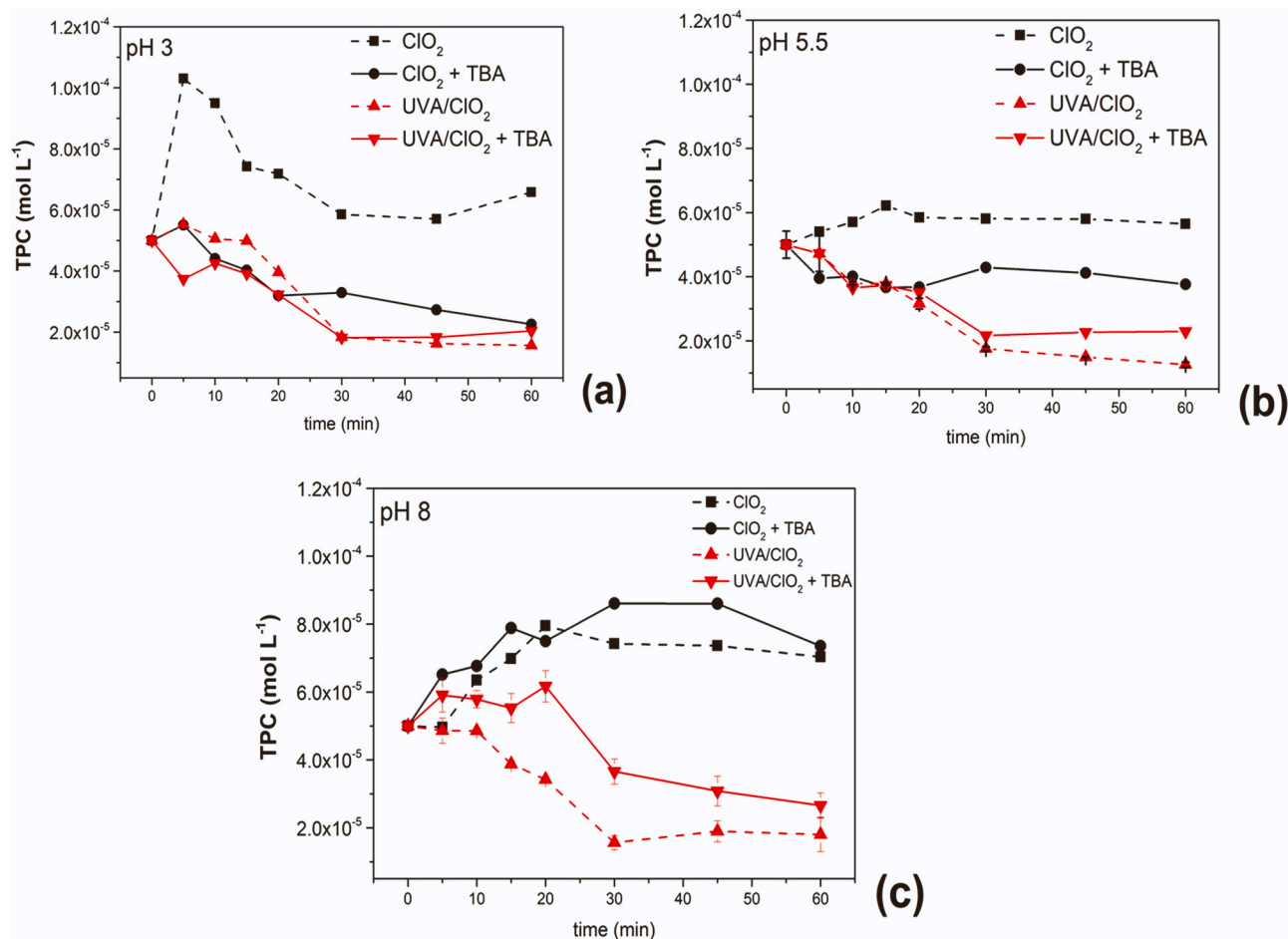
Fig. 7. Total phenolic compounds (TPC) removal during phenol degradation in UVA/ClO_2 processes and in the direct oxidation by ClO_2 in the presence of TBA at pH 3 (a), 5 (b), and 8 (c) ([TBA] = 5.0 × 10^{-3} M, ClO_2/phenol = 20, $[phenol]_0$ = 5.0 × 10^{-5} M, photon flux = 1.26 × 10^{-5} mol_{photon} L^{-1} s^{-1}).

reactions between ClO_2 and phenol or organic matter compounds [23]. In the case of phenol, one mole of FAC was generated after consuming two moles of ClO_2. Chuang et al. (2022) investigated the photolysis of ClO_2 under UVA irradiation and showed the formation of FAC, Cl^-, and ClO_3^- [18]. With the irradiation at 367 nm in UVA/ClO_2 systems, there is no radical formation from FAC via photolysis, as typically observed in UVC/Chlorine processes [49,50], but FAC can contribute to the direct chlorination of organic compounds. In our system, FAC concentrations ranging from 1.4 to 1.8 mg L^{-1} were detected in the absence of organic compounds at pH 3, 5.5, and 8. These species did not undergo photolysis, and about 1 mg L^{-1} of FAC remained in the system after 60 min of exposure to the 367 nm light (Fig S9) (Fig. 8).

Experiments were conducted in the presence of phenol and successive additions of 2 mg L^{-1} of a FAC reagent, replicating the conditions used in the UVA/ClO_2 process. This control experiment showed a high formation of halogenated products, while the TOC removal slightly decreased with the increase of pH, contrary to what happened in the UVA/ClO_2 process (Fig. 8). Therefore, the chlorinated products observed during the degradation of phenol in the UVA/ClO_2 system can also result from the formation of FAC species. Because chlorinated phenols are more resistant to oxidation processes, and FAC species cannot undergo photolysis at the applied wavelength, the observation of higher AOX concentrations was expected. The TOC removal in the presence of FAC is probably associated with the formation of volatile chlorinated compounds.

3.6. The ClO_2^- and ClO_3^- formation and ecotoxicity assay

One of the most significant drawbacks of ClO_2 application is the formation of toxic inorganic by-products, such as ClO_2^- and ClO_3^-, which can increase the toxicity of the treated water [33]. Determination of these by-products is essential when the concentration of ClO_2 is much higher than the practical dose of ClO_2 in water treatment (1–2 mg L^{-1}), mainly used for disinfection. The photolysis of ClO_2 at 365 nm via two product channels results in $ClO\bullet$, $O\bullet$ and $\bullet Cl$ as primary radicals. The formed species participate in complex reactions to generate ClO_2^-, Cl^-, OCl^- and O_3. Some effectively compete for $\bullet OH$ or $\bullet Cl$ and behave as a radical scavenger. Moreover, many of the reactions facilitate the regeneration of ClO_2 [18]. Although ClO_2^- transformation to ClO_3^- is enhanced by UV radiation [51], a recent study reported lower toxicity in UVC/ClO_2 processes than other chlorine-based AOP and UV/H_2O_2 [25].

The ClO_2^- and ClO_3^- concentrations were determined with and without phenol, applying five consecutive additions of 14 ppm ClO_2 (Fig. 7). The sum of the ClO_2^- and ClO_3^- was 38–46% of the total added ClO_2 in each case. Most probably due to the photolysis, the concentration of ClO_2^- decreased by 365 nm radiation, while the ClO_3^- concentration increased significantly, and the molar ratio of ClO_2^-:

ClO_3^- decreased due to the of UV light. Phenol has no significant effect on this molar ratio. It is important to mention that the removal of ClO_2^- can be easily achieved both in bench and in a large scale via the reduction of Fe^{2+} [1]. However, there are no cost-effective solutions for ClO_3^- removal. Therefore, ClO_3^- removal or the decrease in its formation can be considered a challenge for applying the UVA/ClO_2 processes (Fig. 9).

The formation of ClO_2^-, ClO_3^- fro ClO_2, and the chlorine-containing organic compounds from phenol can increase the toxicity of the treated solution. However, the results of the Vibrio Fischer toxicity tests (Table S10) showed no significant increase in toxicity for either the direct ClO_2 oxidation or the ClO_2/UVA method. Nonetheless, increased attention should be paid to the formation of potentially toxic and toxic intermediates in both direct oxidation via ClO_2 and ClO_2/UVA process.

4. Conclusions

The UVA/ClO_2 process performed in a lab-made LED reactor with an emission at 367 nm was proven to be an alternative to the degradation of organic compounds in water. Using COU as a model compound, we observed that the degradation of the organic compounds is strongly affected by pH and the concentration of ClO_2. Successive ClO_2 additions are necessary to promote the degradation of the target compounds, particularly at higher pH values, since the ClO_2 molecule was decomposed in less than five minutes during the tested conditions. We also observed that in the presence of an excess of ClO_2, ideal operational conditions could be achieved at neutral to alkaline pH 5.5–8, and intermediate levels for the LED power.

Using an oxidant/phenol ratio of 20, the removal of total phenolic compounds exceeded 80% at pH 3, 5.5, and 8, and the total organic carbon removal increased with the increase of pH, reaching 47% after 60 min. However, an increase in the percentage of remaining adsorbable chlorinated compounds indicated that these products are more persistent to the degradation than the hydroxylated phenols. The direct oxidation of phenol was less efficient, and about 10% of organic carbon removal was observed for all investigated pH without UV irradiation. Tests in the presence of TBA indicated that the hydroxyl radical participates in the degradation of the substrates in the UVA/ClO_2 system. Still, additional investigations are necessary to assess the contribution of RCS and ROS, which appear to be strongly affected by the pH. The hydroxylation of COU and phenol at pH 8 is probably caused by a direct reaction with ClO_2, not via $HO\bullet$ attack. The monitoring of free available chlorine species indicated their contribution to forming chlorinated products. In summary, the UVA/ClO_2 process was advantageous for removing and mineralizing phenol and COU compared to direct oxidation. Still, this process needs to be improved or coupled with other steps to minimize the formation of chlorinated organic products and ClO_3^- as toxic products.
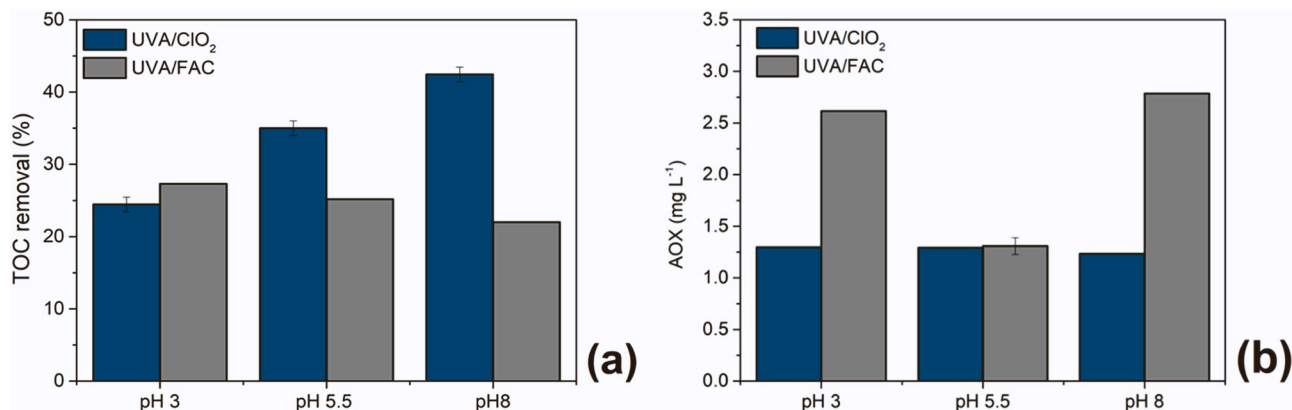
Fig. 8. Comparison of the TOC removal (a), and AOX concentration (b) determined after 60 min during phenol degradation in UVA/ClO_2 and UVA/FAC processes ([phenol]$_0$ = 5×10^{-5} M, $5 \times$[FAC] = 2.8×10^{-5} M (2 mg L^{-1}), $5 \times$ [ClO_2] = 2.08×10^{-4} M (14 mg L^{-1}), photon flux = 1.26×10^{-5} mol$_{photon}$ L^{-1} s^{-1}).
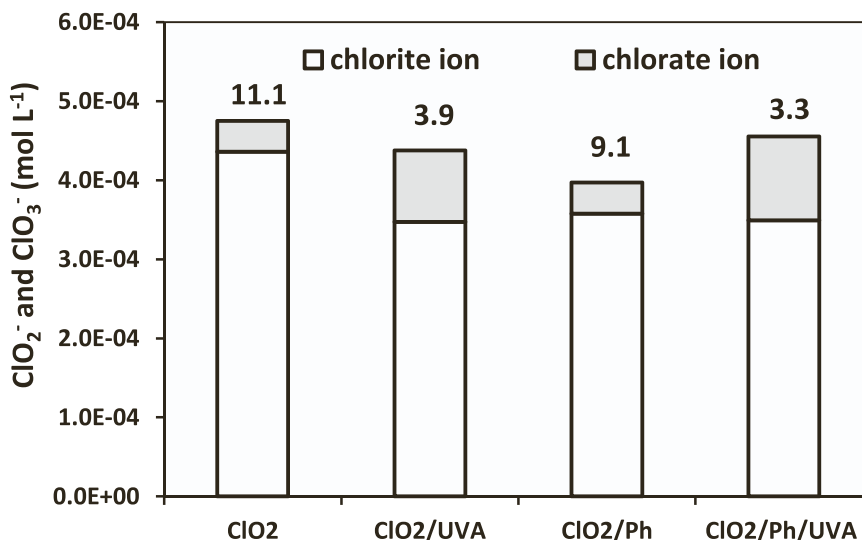
Fig. 9. The concentration of ClO_2^- and ClO_3^- and the ClO_2^-:ClO_3^- concentration ratio (the value at the top of the column) after five consecutive additions of 14 ppm ClO_2. (ClO_2/phenol = 20; $5 \times [ClO_2]_0 = 2.08 \times 10^{-4}$ M (14 mg L^{-1}), $[phenol]_0 = 5 \times 10^{-5}$ M, photon flux $= 1.26 \times 10^{-5}$ mol$_{photon}$ L^{-1} s^{-1}).

CRediT authorship contribution statement

Daniele Scheres Firak: Investigation, Formal analysis, Writing – original draft, Writing – review & editing. **Luca Farkas:** Investigation, chromatography measurements. **Máté Náfrádi:** Investigation. **Tünde Alapi:** Conceptualization, Methodology, Resources, Writing – review & editing.

Declaration of Competing Interest

The authors declare that they have no known competing financial interests or personal relationships that could have appeared to influence the work reported in this paper.

Acknowledgments

Appendix A. Supporting information

Supplementary data associated with this article can be found in the online version at doi:10.1016/j.jece.2022.107554.

References

[1] B.& Veatch, Corporation. White's Handbook of Chlorination and Alternative Disinfectants, John Wiley & Sons, Hoboken, New Jersey, 2010.

[2] H. Gallard, U. von Gunten, Chlorination of phenols: kinetics and formation of chloroform, Environ. Sci. Technol. 36 (2002) 884–890, https://doi.org/10.1021/es010076a.

[3] F. Ge, L. Zhu, J. Wang, Distribution of chlorination products of phenols under various pHs in water disinfection, Desalination 225 (2008) 156–166, https://doi.org/10.1016/j.desal.2007.03.016.

[4] J. Terhalle, P. Kaiser, M. Jütte, J. Buss, S. Yasar, R. Marks, H. Uhlmann, T. C. Schmidt, H.V. Lutze, Chlorine dioxide - pollutant transformation and formation of hypochlorous acid as a secondary oxidant, Environ. Sci. Technol. 52 (2018) 9964–9971, https://doi.org/10.1021/acs.est.8b01099.

[5] R. ya Jin, S. qi Hu, Y. ghao Zhang, T. Bo, Concentration-dependence of the explosion characteristics of chlorine dioxide gas, J. Hazard. Mater. 166 (2009) 842–847, https://doi.org/10.1016/j.jhazmat.2008.11.124.

[6] J. Marcon, G. Mortha, N. Marlin, F. Molton, C. Duboc, A. Burnet, New insights into the decomposition mechanism of chlorine dioxide at alkaline pH, Holzforschung 71 (2017) 599–610, https://doi.org/10.1515/hf-2016-0147.

[7] D.R. Svenson, J.F. Kadla, H. min Chang, H. Jameel, Effect of pH on the inorganic species involved in a chlorine dioxide reaction system, Ind. Eng. Chem. Res. 41 (2002) 5927–5933, https://doi.org/10.1021/ie020191.

[8] M. Medir, F. Giralt, Stability of chlorine dioxide in aqueous solution, Water Res. 16 (1982) 1379–1382, https://doi.org/10.1016/0043-1354(82)90221-4.

[9] M.V. Pergal, I.D. Kodranov, M.M. Pergal, B.P. Dojčinović, D.M. Stanković, B. B. Petković, D.D. Manojlović, Assessment of degradation of sulfonylurea herbicides in water by chlorine dioxide, Water Air Soil Pollut. 229 (2018), https://doi.org/10.1007/s11270-018-3947-2.

[10] T.Y. Zhang, B. Xu, C.Y. Hu, Y.L. Lin, L. Lin, T. Ye, F.X. Tian, A comparison of iodinated trihalomethane formation from chlorine, chlorine dioxide and potassium permanganate oxidation processes, Water Res. 68 (2015) 394–403, https://doi.org/10.1016/j.watres.2014.09.040.

[11] Y. Lee, U. von Gunten, Oxidative transformation of micropollutants during municipal wastewater treatment: Comparison of kinetic aspects of selective (chlorine, chlorine dioxide, ferrateVI, and ozone) and non-selective oxidants (hydroxyl radical), Water Res. 44 (2010) 555–566, https://doi.org/10.1016/j.watres.2009.11.045.

[12] W. Gan, Y. Ge, Y. Zhong, X. Yang, The reactions of chlorine dioxide with inorganic and organic compounds in water treatment: kinetics and mechanisms, Environ. Sci. Water Res. Technol. 6 (2020) 2287–2312, https://doi.org/10.1039/d0ew00231c.

[13] J.J. Lin, D.W. Hwang, Y.T. Lee, X. Yang, Photodissociation dynamics of OClO at 157 nm, J. Chem. Phys. 108 (1998) 10061–10069, https://doi.org/10.1063/1.476466.

[14] T.J. Bixby, J.C. Bolinger, J.D. Patterson, P.J. Reid, Femtosecond pump-probe studies of actinic-wavelength dependence in aqueous chlorine dioxide photochemistry, J. Chem. Phys. 130 (2009) 1–11, https://doi.org/10.1063/1.3116108.

[15] P.J. Reid, Investigating the phase-dependent reactivity of chlorine dioxide using resonance Raman spectroscopy, J. Phys. Chem. A 106 (2002) 1473–1482, https://doi.org/10.1021/jp013491y.

[16] F. Tian, W. Ye, B. Xu, X. Hu, S. Ma, F. Lai, Y. Gao, H.-B. Xing, W.-H. Xia, B. Wang, Comparison of UV-induced AOPs (UV/Cl, UV/NHCl, UV/ClO and UV/HO) in the degradation of iopamidol: kinetics, energy requirements and DBPs-related toxicity in sequential disinfection processes, Chem. Eng. J. 398 (2020), 125570, https://doi.org/10.1016/j.cej.2020.125570.

[17] M.J. Philpott, S.C. Hayes, P.J. Reid, Femtosecond pump-probe studies of chlorine dioxide photochemistry in water and acetonitrile, Chem. Phys. 236 (1998) 207–224, https://doi.org/10.1016/S0301-0104(98)00204-3.

[18] Y.-H. Chuang, K.-L. Wu, W.-C. Lin, H.-J. Shi, Photolysis of chlorine dioxide under UVA irradiation: radical formation, application in treating micropollutants, formation of disinfection byproducts, and toxicity under scenarios relevant to potable reuse and drinking water, Environ. Sci. Technol. (2022), https://doi.org/10.1021/acs.est.1c05707.

[19] N. Kishimoto, State of the art of UV/chlorine advanced oxidation processes: their mechanism, byproducts formation, process variation, and applications, J. Water Environ. Technol. 17 (2019) 302–335, https://doi.org/10.2965/jwet.19-021.

[20] Z. Wu, K. Guo, J. Fang, X. Yang, H. Xiao, S. Hou, X. Kong, C. Shang, X. Yang, F. Meng, L. Chen, Factors affecting the roles of reactive species in the degradation

of micropollutants by the UV/chlorine process, Water Res. 126 (2017) 351–360, https://doi.org/10.1016/j.watres.2017.09.028.

[21] J. Fang, Y. Fu, C. Shang, The roles of reactive species in micropollutant degradation in the UV/free chlorine system, Environ. Sci. Technol. 48 (2014) 1859–1868, https://doi.org/10.1021/es4036094.

[22] Q. Kong, X. Lei, X. Zhang, S. Cheng, C. Xu, B. Yang, X. Yang, The role of chlorine oxide radical (ClO•) in the degradation of polychoro-1,3-butadienes in UV/chlorine treatment: kinetics and mechanisms, Water Res. 183 (2020), 116056, https://doi.org/10.1016/j.watres.2020.116056.

[23] V. Rougé, S. Allard, J.P. Croué, U. Von Gunten, In situ formation of free chlorine during ClO2 treatment: implications on the formation of disinfection byproducts, Environ. Sci. Technol. 52 (2018) 13421–13429, https://doi.org/10.1021/acs.est.8b04415.

[24] Q. Kong, M. Fan, R. Yin, X. Zhang, Y. Lei, C. Shang, X. Yang, Micropollutant abatement and byproduct formation during the co-exposure of chlorine dioxide (ClO$_2$) and UVC radiation, J. Hazard. Mater. 419 (2021), 126424, https://doi.org/10.1016/j.jhazmat.2021.126424.

[25] W.K. Ye, F.X. Tian, B. Xu, D.S. Zhao, J. Ye, B. Wang, F. Lai, Y.J. Tan, X.J. Hu, Insights into the enhanced degradation of flumequine by UV/ClO2 integrated process: kinetics, mechanisms and DBPs-related toxicity in post-disinfection, Sep. Purif. Technol. 280 (2022), 119846, https://doi.org/10.1016/j.seppur.2021.119846.

[26] M. Martín-Sómer, C. Pablos, R. van Grieken, J. Marugán, Influence of light distribution on the performance of photocatalytic reactors: LED vs mercury lamps, Appl. Catal. B Environ. 215 (2017) 1–7, https://doi.org/10.1016/j.apcatb.2017.05.048.

[27] S.E. Beck, H. Ryu, L.A. Boczek, J.L. Cashdollar, K.M. Jeanis, J.S. Rosenblum, O. R. Lawal, K.G. Linden, Evaluating UV-C LED disinfection performance and investigating potential dual-wavelength synergy, Water Res. 109 (2017) 207–216, https://doi.org/10.1016/j.watres.2016.11.024.

[28] K. Song, M. Mohseni, F. Taghipour, Application of ultraviolet light-emitting diodes (UV-LEDs) for water disinfection: a review, Water Res. 94 (2016) 341–349, https://doi.org/10.1016/j.watres.2016.03.003.

[29] R. Xiong, Z. Lu, Q. Tang, X. Huang, H. Ruan, W. Jiang, Y. Chen, Z. Liu, J. Kang, D. Liu, UV-LED/chlorine degradation of propranolol in water: degradation pathway and product toxicity, Chemosphere 248 (2020), 125957, https://doi.org/10.1016/j.chemosphere.2020.125957.

[30] I. Carra, J. Fernandez Lozano, O. Autin, J.R. Bolton, P. Jarvis, Disinfection by-product formation during UV/Chlorine treatment of pesticides in a novel UV-LED reactor at 285 nm and the mitigation impact of GAC treatment, Sci. Total Environ. 712 (2020), 136413, https://doi.org/10.1016/j.scitotenv.2019.136413.

[31] J. Chen, S. Loeb, J.H. Kim, LED revolution: fundamentals and prospects for UV disinfection applications, Environ. Sci. Water Res. Technol. 3 (2017) 188–202, https://doi.org/10.1039/c6ew00241b.

[32] X. Kong, J. Jiang, J. Ma, Y. Yang, S. Pang, Comparative investigation of X-ray contrast medium degradation by UV/chlorine and UV/H2O2, Chemosphere 193 (2018) 655–663, https://doi.org/10.1016/j.chemosphere.2017.11.064.

[33] World Health Organization, Guidelines for drinking-water quality: fourth edition incorporating the first addendum, (2017).

[34] C. Tan, Q. Xu, H. Zhang, Z. Liu, S. Ren, H. Li, Enhanced removal of coumarin by a novel O3/SPC system: kinetic and mechanism, Chemosphere 219 (2019) 100–108, https://doi.org/10.1016/j.chemosphere.2018.11.194.

[35] W. Liu, C. Fang, Y. Huang, L. Ai, F. Yang, Z. Wang, J. Liu, Is UV/Ce(IV) process a chloride-resistant AOPs for organic pollutants decontamination? RSC Adv. 6 (2016) 93558–93563, https://doi.org/10.1039/c6ra21682j.

[36] J.E. Wajon, D.H. Rosenblatt, E.P. Burrows, Oxidation of phenol and hydroquinone by chlorine dioxide, Environ. Sci. Technol. 16 (1982) 396–402, https://doi.org/10.1021/es00101a006.

[37] I.M. Ganiev, E.S. Suvorkina, N.N. Kabal'nova, Reaction of chlorine dioxide with phenol, Russ. Chem. Bull. 52 (2003) 1123–1128, https://doi.org/10.1023/A:1024905223801.

[38] TwinOxide, TwinOxide products 0.3% Chlorine Dioxide, (2022). ⟨https://www.twinoxide.com/products/twinoxide-03-chlorine-dioxide/⟩. (Accessed June 25, 2021).

[39] J.D. Box, Investigation of the Folin-Ciocalteau phenol reagent for the determination of polyphenolic substances in natural waters, Water Res. 17 (1983) 511–525, https://doi.org/10.1016/0043-1354(83)90111-2.

[40] Y. Nosaka, A.Y. Nosaka, Generation and detection of reactive oxygen species in photocatalysis, Chem. Rev. 117 (2017) 11302–11336, https://doi.org/10.1021/acs.chemrev.7b00161.

[41] Y. Nosaka, A.Y. Nosaka, Comment on "Coumarin as a quantitative probe for hydroxyl radical formation in heterogeneous photocatalysis, J. Phys. Chem. C 123 (2019) 20682–20684, https://doi.org/10.1021/acs.jpcc.9b04190.

[42] H. Czili, A. Horváth, Applicability of coumarin for detecting and measuring hydroxyl radicals generated by photoexcitation of TiO2 nanoparticles, Appl. Catal. B Environ. 81 (2008) 295–302, https://doi.org/10.1016/j.apcatb.2008.01.001.

[43] G. Louit, S. Foley, J. Cabillic, H. Coffigny, F. Taran, A. Valleix, J.P. Renault, S. Pin, The reaction of coumarin with the OH radical revisited: hydroxylation product analysis determined by fluorescence and chromatography, Radiat. Phys. Chem. 72 (2005) 119–124, https://doi.org/10.1016/j.radphyschem.2004.09.007.

[44] M. Náfrádi, L. Farkas, T. Alapi, K. Hernádi, K. Kovács, L. Wojnárovits, E. Takács, Application of coumarin and coumarin-3-carboxylic acid for the determination of hydroxyl radicals during different advanced oxidation processes, Radiat. Phys. Chem. 170 (2020), https://doi.org/10.1016/j.radphyschem.2019.108610.

[45] K. Gopakumar, U.R. Kini, S.C. Ashawa, N.S. Bhandari, G.U. Krishnan, D. Krishnan, Gamma irradiation of coumarin in aqueous solution, Radiat. Eff. 32 (1977) 199–203, https://doi.org/10.1080/00337577708233075.

[46] G. Louit, S. Foley, J. Cabillic, H. Coffigny, F. Taran, A. Valleix, J.P. Renault, S. Pin, The reaction of coumarin with the OH radical revisited: Hydroxylation product analysis determined by fluorescence and chromatography, Radiat. Phys. Chem. 72 (2005) 119–124, https://doi.org/10.1016/j.radphyschem.2004.09.007.

[47] G. Žerjav, A. Albreht, I. Vovk, A. Pintar, Revisiting terephthalic acid and coumarin as probes for photoluminescent determination of hydroxyl radical formation rate in heterogeneous photocatalysis, Appl. Catal. A Gen. 598 (2020), https://doi.org/10.1016/j.apcata.2020.117566.

[48] Y. Huang, B. Sheng, F. Yang, Z. Wang, Y. Tang, Q. Liu, X. Wang, J. Liu, Chlorine incorporation into dye degradation by-product (coumarin)in UV/peroxymonosulfate process: a negative case of end-of-pipe treatment, Chemosphere 229 (2019) 374–382, https://doi.org/10.1016/j.chemosphere.2019.05.024.

[49] C. Sichel, C. Garcia, K. Andre, Feasibility studies: UV/chlorine advanced oxidation treatment for the removal of emerging contaminants, Water Res. 45 (2011) 6371–6380, https://doi.org/10.1016/j.watres.2011.09.025.

[50] M. Li, M. Hao, L. Yang, H. Yao, J.R. Bolton, E.R. Blatchley, Z. Qiang, Trace organic pollutant removal by VUV/UV/chlorine process: feasibility investigation for drinking water treatment on a mini-fluidic VUV/UV photoreaction system and a pilot photoreactor, Environ. Sci. Technol. 52 (2018) 7426–7433, https://doi.org/10.1021/acs.est.8b00611.

[51] J. Wang, J. Wu, L. Bu, S. Zhu, W. Zhang, S. Zhou, N. Gao, Simultaneous removal of chlorite and contaminants of emerging concern under UV photolysis: hydroxyl radicals vs. chlorate formation, Water Res. 190 (2021), 116708, https://doi.org/10.1016/j.watres.2020.116708.